International Journal of Applied Engineering Research ISSN 0973-4562 Volume 13, Number 6 (2018) pp. 375-385

Numerical Analysis of different blade profile of wind turbine

Gaurav Kumar*, Vipin, Raja Ram , Neeraj Kumar
Assistant Professor, Department of Mechanical Engineering,
KIET Group of Institutions, Ghaziabad, India.

Abstract
A comparative study of the classical savonius rotor with semicircular blades and a new blade configuration has been done using ANSYS Fluent 14.0. The variation in dynamic torque and power coefficient with respect to the tip speed ratio of the rotors have been systematically analyzed. The self starting capability of the rotor is assessed by studying the static torque exerted on the rotors at various angles with respect to wind velocity. The optimal blade profile was identified by examining the performance characteristics of each geometry under study. The most favorable design was also found to be capable of self starting at any rotor angle with respect to wind velocity. The idea behind the new design was to harvest the incoming wind to generate a wind jet to concave side of the advanced blade and prevent the convex side of the returning blade from coming upwind stream by guiding it through different guide plates, to impinge the concave side of return blade and hence to eliminate the negative torque. The research reflected using structured grid under k-w SST turbulent modeling in transient conditions for 2-D modeling under dynamic mode, is a method of great accuracy to generate numerical data that follows closely the experimental curve. So the models were studied in k-w SST transient turbulent model under dynamic conditions. The result showed that the suggested designs improve performance of savonius rotor in view of the power coefficient and the operating range. The performance achieved with one of the suggested guide plate design in terms of power coefficient is 0.14 for tip speed ratio 0.8. With the use of suggested designs of guide plate, the model can be operated even at higher tip speed ratio.

Keywords: Power coefficient; Savonius; Static torque; Tip speed ratio

INTRODUCTION

Wind power harvesting with the help of wind turbine is a new and an emerging field in power generation. With the intention of using this abundant source of wind energy, various designs of wind turbine have been proposed till date. However, only few have been found to be practically suitable and useful. Depending on their axis of rotation wind turbines are mainly two types - horizontal axis wind turbine (HAWT) and vertical axis wind turbine (VAWT). HAWTs are very well-known for their comparatively high efficiency over VAWTs and inherently have been used for electricity production. Multi blade type and propeller type are few HAWTs. However, the VAWTs have significant advantages over HAWTs such as simple in construction, lower installation and maintenance cost, good self-starting capability, independent of the wind direction and no need of over speed control etc. These advantages are confirming the use of VAWT for small scale applications [5]. VAWTs can be further classified into various categories such as Savonius and Darrieus rotor etc. Fig.1 represents different types of wind turbine rotors.

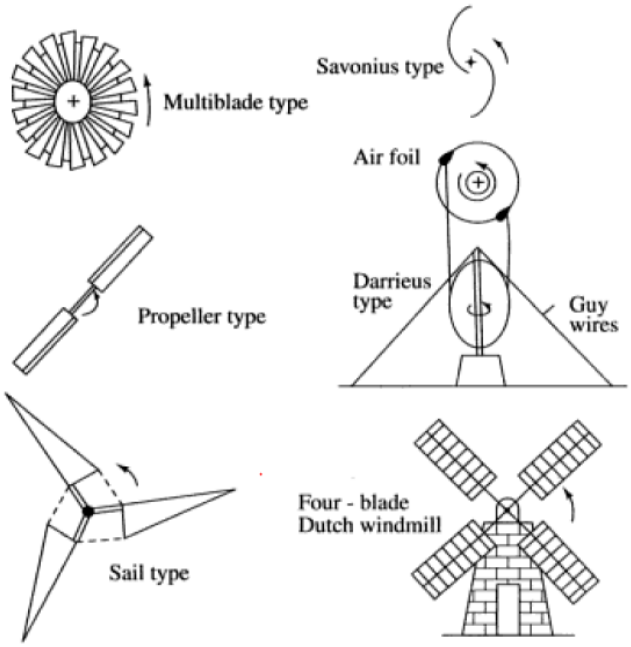

Figure 1: Types of wind turbine rotors

Among this VAWTs, Savonius rotors offer an easy way to harness this vast wind power for small scale applications because of their simple construction and wind direction independence. This class of turbine is a very useful device for water pumping in agricultural purposes, especially in rural areas where the water level is within a distance of 5 m below the ground. The installation and maintenance costs are very low and it can be installed on rooftops for local electricity production.

The Savonius rotor turbine is designed to be driven by the drag effect of wind on the turbine blade and that is why known as drag type rotors. The top view of Savonius rotor is somewhat analogous to "S" shape. It is simple in structure, have a very low cut-in speed and accepts wind from any direction (Ross and Altman, 2011) [19].The conventional Savonius wind rotor is made by cutting a cylinder into two halves, along its central axis an relocating the two semi-cylindrical airfoils sideways as

shown in Fig.2. The semi cylindrical airfoils are called blades which are used to convert the kinetic energy of the wind into electrical energy.

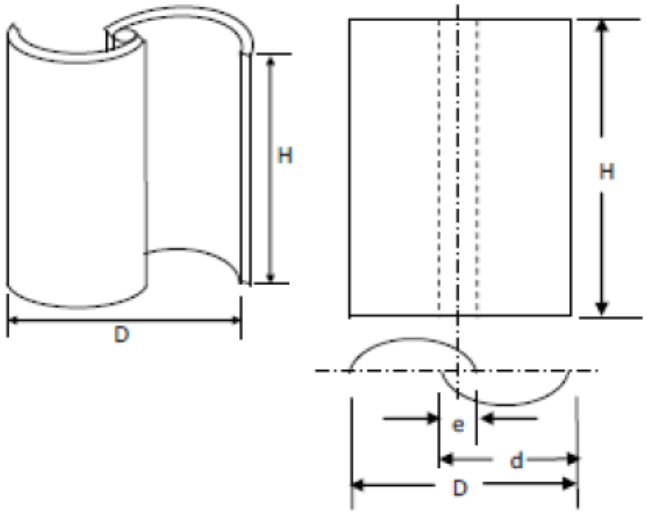

Figure 2: Two bladed Savonius rotor

It was originally introduced by a Finish engineer named savonius in the 1920s (Paraschivoiu, 2002) [18] and basically is a modification of the flettner's rotor used in ships. It has low noise emissions because of low rotational speed. Its mechanical and aerodynamic characteristics make it suitable for the high turbulence intensity experienced in the urban area. Atypical conventional Savonius style turbine possesses a power conversion efficiency of 12%-20% which is relatively lesser in comparison with Darrieus style turbine. Nevertheless, it is worth mentioning that if we modified the design of savonius style turbines, this peak power conversion efficiency can be increased upto 30%-35% (Shepherd and Zhang,2011;Abraham et al.2012; Akwa et al. 2012). The conventional Savonius rotor has a high starting torque and this is an advantage for particularity this kind of wind turbine (Hayashi et al, 2005), as they are often applied for starting torques for other VAWTs (Chauvin and Benghrib, 1989) [8]. This devices are insensitive to the wind flow directions, and thus, are very useful for the specific locations of variable wind directions. The vertical rotational axis allows them to be positioned in confined space or atop buildings (Abraham et al. 2012; Akwa et al. 2012). A Savonius rotor designed with three blades generates favorable torque characteristics. However, it has a poor maximum power coefficient compared to the VAWT with two blades (Ross and Altman, 2011). So the number of rotor blades has a direct impact on the rotor performance (Al-Bahadly, 2009) [1]. Menet (2004) [15] affirmed that a two-stage Savonius rotor develops improved torque and power coefficients in comparison to the rotor in a single stage (Akwa et al, 2012). In the present work, a Savonius rotor with two blades and a single stage is modeled for simplicity of the rotor geometry and because it is the most commonly-studied type of Savonius rotor.

Problem Formulation

The problem was developed to study the aerodynamic characteristics of the various shapes of Savonius rotors and compare the result obtained for 2-D models using unsteady analysis. Also the research was taken ahead on the optimal blade profile by using two newly designed guide plates and the aerodynamic characteristics were studied under the same conditions.

The basic mathematical formulations required to study the aerodynamics of Savonius rotors under unsteady conditions are:-

Average Coefficient of power, $C_P = \frac{P}{0.5\rho AU^3}$

Tip Speed Ratio, $\lambda = \frac{\omega R}{U}$

Aspect Ratio, $\alpha = \frac{H}{D}$

Average Coefficient of Torque, $C_m = \frac{M}{\rho ARU^2}$

The governing equations that were solved during the simulations are:

(a) The continuity equation:

$$\frac{\partial \rho}{\partial t} + \frac{\partial (\rho u)}{\partial x} + \frac{\partial (\rho v)}{\partial y} + \frac{\partial (\rho w)}{\partial z} = 0$$

The first term in the left hand side of the equation is zero here, because we have assumed the density of the fluid (air) is constant in the entire simulation.

(b) The momentum equations:

$$\rho \frac{Du}{Dt} = \rho g - \frac{\partial \rho}{\partial x} + \mu \left(\frac{\partial^2 u}{\partial x^2} + \frac{\partial^2 v}{\partial y^2} + \frac{\partial^2 w}{\partial z^2} \right)$$

$$\rho \frac{Dv}{Dt} = \rho g - \frac{\partial \rho}{\partial y} + \mu \left(\frac{\partial^2 u}{\partial x^2} + \frac{\partial^2 v}{\partial y^2} + \frac{\partial^2 w}{\partial z^2} \right)$$

$$\rho \frac{Dw}{Dt} = \rho g - \frac{\partial \rho}{\partial z} + \mu \left(\frac{\partial^2 u}{\partial x^2} + \frac{\partial^2 v}{\partial y^2} + \frac{\partial^2 w}{\partial z^2} \right)$$

Physical Model

The computational model for the Elliptical Savonius rotor is made by slicing off a section of a Ellipse by a plane inclined at particular angle to its major axis as shown in Fig. 3.

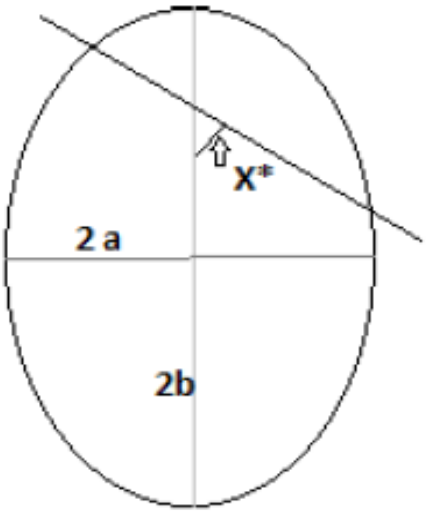

Figure 3: Sectional cut on an ellipse

The dimensions of ellipse are taken as a/b = 2/3 such that the overall diameter of the rotor obtained as 0.542 m. Various elliptical bladed Savonius rotors are made by sectioning the ellipse having major axis 3 m and minor axis 2 m by the planes inclined at various an angle x^*, with the vertical plane, where x is 30°,40°,50°,60° so that we are able to get the desired blade profile. The reason for choosing the above dimension of the ellipse was, to get the blades with chord length of 0.5426 m, which is identical to all elliptical Savonius rotors. The size of the computational domain is selected in such a way that the results are not affected by the boundaries of domain. The blade overlap distance for all the cases is taken as 20% of the blade chord length.

Simulation Model

The flow around the SSWTs is assumed to be fully unsteady and turbulent, operating at a free stream wind speed of 6.2 m/s. The dynamic simulations are carried out by assigning a certain rotational rate (ω in rad/s) to the rotating zone. To predict the performance of the turbine in terms of torque coefficient (C_t) and power coefficient (C_p) with respect to TSR. The SST k-ω turbulence model is found to be suitable for analysis as compared to other turbulence models. It is due to fact that the SST k-ω turbulence model is a blended model of k-ω and k-ϵ turbulence models. The reason for the selection of this model was, its better accuracy with practical results as is mentioned in the literature (Afungchui et al., 2010: D¨Alessandro et al., 2010; Akwa et al., 2012). SST *k-ω* model is also known to give highly accurate predictions of flow separation under adverse pressure by an implementation of the transport effects on the formulation of the eddy viscosity (Sargolzai and Kainifer, 2009). So, it is utilized whenever a high boundary layer accuracy is required, which is the case in these investigations.

The spatial discretization of the conservative equations is treated with 2nd order upwind scheme and the temporal terms of the conservative equations are discretized using 1st order fully implicit temporal scheme. Good solution stability is ensured through the pressure- velocity coupling with the SIMPLE method (Semi Implicit Linked Equations). For the solution iteration, the time step size and the number of iterations per time step are taken as 0.01 and 20, respectively.

Boundary Condition

Once the meshing is accomplished, the boundary conditions are assigned to the domain. The inlet is given as velocity inlet (V= 6.2 m/s), outlet as pressure outlet (atmospheric pressure), turbine models as no-slip boundary condition, and the rotating zone is assigned as a sliding mesh at a certain rotational speed with respect to TSR. The upper and bottom side of the domain is assumed to be symmetry boundary conditions. As shown in Fig.4.

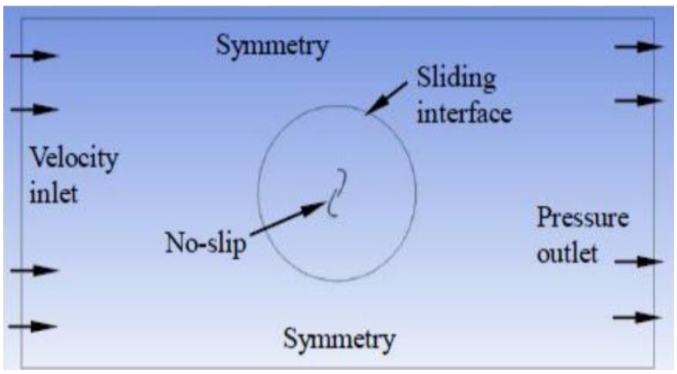

Figure 4: Boundary Conditions

For Designs of Guide Plates

For further study, two designs of guide plates are proposed as shown in Fig. 5.

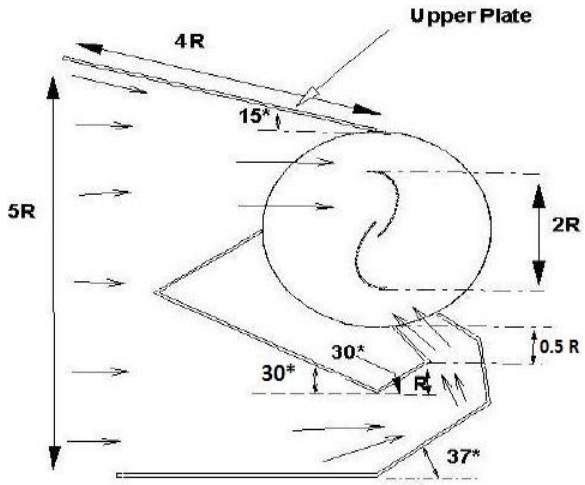

Design A

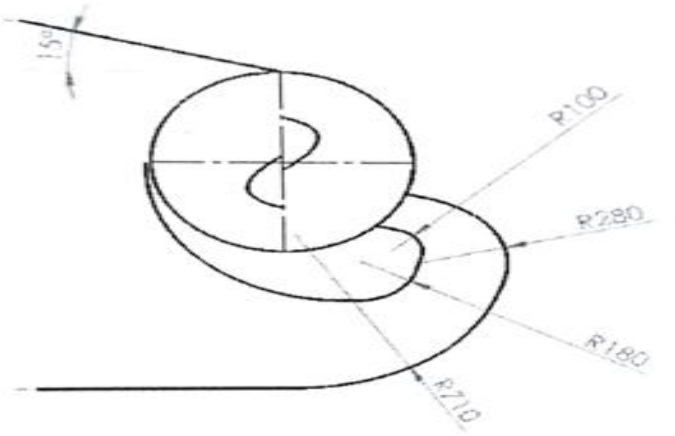

Design B

Figure 5: Designs of guide blade

In both the designs, the upper plates are proposed as shown in Fig. 5. In both the designs, the upper plate is inclined with 15 degree to horizontal as suggested by (Altan and Atilgan 2010). The length of the upper plate is kept as 4R in order to give sufficient developing length and hence reducing entrance effects.

The upper plate is aimed to collect more amount of wind and generate a jet to the concave side of the blade. The lower part of the design B has collection area greater than the design A. The exit jet from the lower passage has width of 0.5R for both the designs. The position of the exit jet centre has a distance 0.75R for design A and 1.25R for design B. The exit jet position is selected to prevent the convex side of returning plate from generating negative torque at rotor angle between 90 and 170 degree.

Details of Domain Discretization

The computational domain is discretized using unstructured domain by using quad cells to solve the equations using finite volume method(FVM). An overview of computational domain n is shown in Fig.4, It consist of two parts: the first part is fixed mesh and the other is rotating mesh. The rotating mesh is bounded by the interface of both the parts. The rotating region has diameter of 0.8 m and place in the centre of the domain. The dimension of domain is 7m×4m. Near the blades, fine layer are adjusted in order to capture the flow properties near blade surfaces. The minimum size of each cell is fixed as 0.001m for all the models. There is uniform concentration of cells at the interface of stator and rotor.

A grid independence study is carried in between triangular cells and quadrilateral cells to approach the realizable grid distances and good resolution that produces reasonable computational results and found quadrilateral cells as more competitive as shown in Fig. 6 and Fig. 7. Mesh refinement was done to model the geometry of the Savonius rotors and no noticeable variations are noticed in the final solutions with increasing the number of cells.

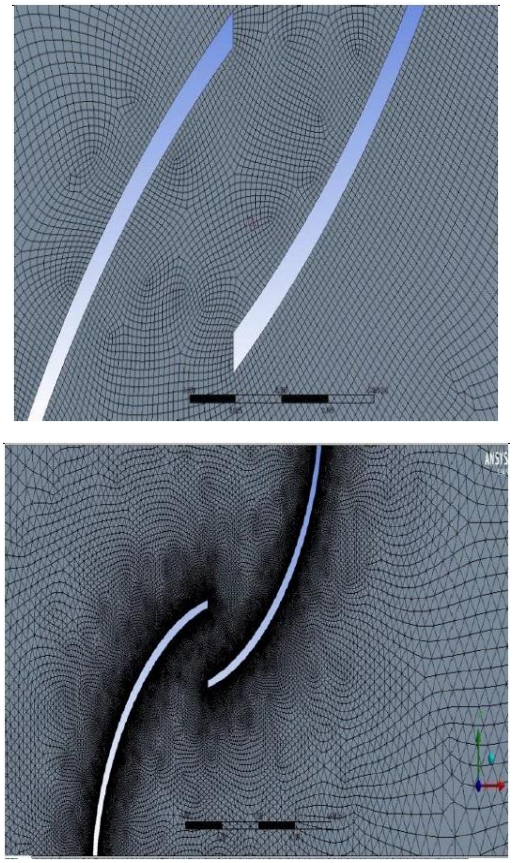

Figure 7: Triangular mesh near blade profile

RESULTS AND DISCUSSION

With the SST k-ω turbulence model, at 6.2 m/s, 2D unsteady simulations were carried out on all the elliptical blades. After finding the optimal blade profile, using different guide plates unsteady simulation were again carried out. Fig.8 shows the torque coefficient respectively at different TSR for Elliptical savonius rotor and the new designs also. It indicates a gradual decrease in C_t as rotational speed increases. From the figures, it is clear that design B has the highest value torque coefficient compared with 50° elliptical blade and the other design. The static torque coefficient increases with high values in the range of rotor angle of 90°-135° for both the guide plates because the generated wind jet in the new designs impinge into the concave side of the return blades.

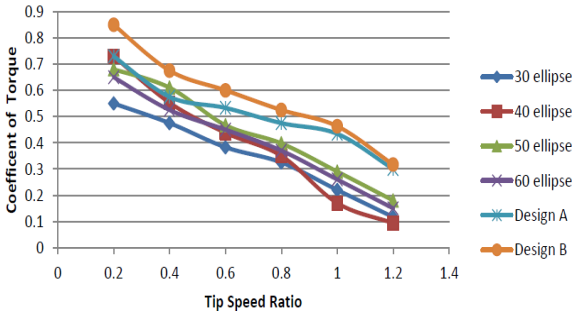

Figure 8: Variation of Torque Coefficient with Tip Speed Ratio for elliptical blade profile

The variation of the coefficient of power has also been studied for all the 2-D elliptical style rotors as well as for rotor with new guide plates by varying the tip speed ratio under transient dynamic mode and unsteady *k-ω* turbulent model. The comparison of the numerical values of coefficient of power of elliptical rotors along with the both the guide plates with respect to tip speed ratio, has been shown in Fig. 9. it is clear that the rotor using guide plate design B has highest value of power coefficient when compared to other rotors. The directed wind harvested in the passage of design B includes a smooth turning and hence, a reduction of the lost energy compared with the design A.

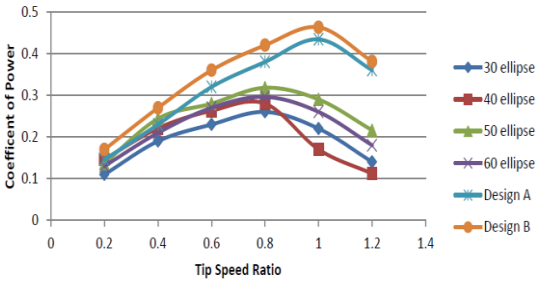

Figure 9: Variation of Power Coefficient with Tip Speed Ratio for elliptical blade profile

Table 1: Comparison of numerical data for 2-D Various elliptical-bladed Savonius rotors

Tip Speed Ratio	*Coefficient*	*Of*	*Power*	
	30° elliptical Savonius Rotor	*40° elliptical Savonius Rotor*	*50° elliptical Savonius rotor*	*60° elliptical Savonius rotor*
0.2	0.11	0.146	0.136	0.13
0.4	0.19	0.221	0.244	0.21
0.6	0.23	0.263	0.28	0.27
0.8	0.26	0.28	0.318	0.296
1.0	0.22	0.17	0.29	0.26
1.2	0.14	0.112	0.216	0.18

Table 2: Effect of Guide plates designs on C p of elliptical savonius rotors

Tip speed Ratio	Coefficient of power		
	Rotor without guide plates	Rotor with Guide plate A	Rotor with guide plate B
0.2	0.136	0.146	0.17
0.4	0.244	0.23	0.27
0.6	0.28	0.32	0.36
0.8	0.318	0.38	0.42
1.0	0.29	0.434	0.463
1.2	0.216	0.36	0.38

Three blade profiles have been selected for study 1. 50º elliptical blade profile 2. Semi-circular blade profile 3. Novel blade profile

The classical semi-circular blade configuration is depicted in fig:-6. Describing the important geometrical factors. The modified blade novel configuration is shown in fig:-7 is featured by spline connecting a set of three characteristic points as used by Nilavarasan and Dheenadhayalan [22]. The terminal points of blade viz., A(0.03m, 0m) and C(-0.2m, 0m) remain unaltered. The third characteristic point B, which is chosen on the tangent to the semi- circle at a point where the height from the diameter is the radius and coordinates are B(-0.14m, 0.1m). The common geometrical parameters of the rotor geometry under study have been presented in Fig. 11.

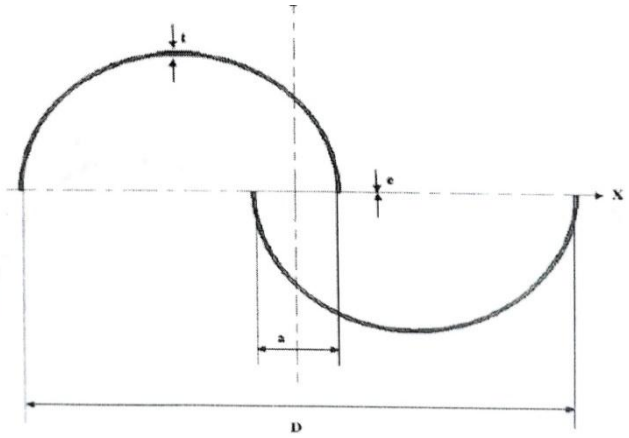

Figure 10: Semi-circular profile

Figure 11: Modified novel profile

Velocity Flow Field (Elliptical Profile)

The velocity flow field has a complex flow structure. The presence of re-circulating zone can be seen in the rotors. The presence of overlap jet is also found in the rotors, which is more significant in the 50° elliptic Savonius rotor. This overlap jet causes the negative contribution of the returning blade to the overall torque of the turbine, which is significantly reduced.

From the contours, that the flow separation, flow stagnation, and the formation of vortices are responsible for the variation in the average power of the Savonius rotors. We can predict that the

flow separation take place near the tip of the advancing blade causes the vortices to form at the down streams of the turbine blades.

After study the optimal blade profile, velocity flow field of savonius rotor using guide plates designs were also studied. Fig. 16 and Fig. 17 shows the velocity contours around the rotor with the design A and design B respectively at rotor angle 135°. It can be noticed that strong wakes behind the rotor are generated. The upstream wind enters the designs from two stream; one generates the first wind jet to the concave side of advancing blade and the other generates the second wind jet to the concave side of returning blade. The flow direction guiding of such design is of course a subsidizing tool to generate a strong active momentum which is responsible for enhancing the generated torque from such new design. When comparing both the designs, one can observe the design B generates asymmetric large wakes with strong vortex shedding.

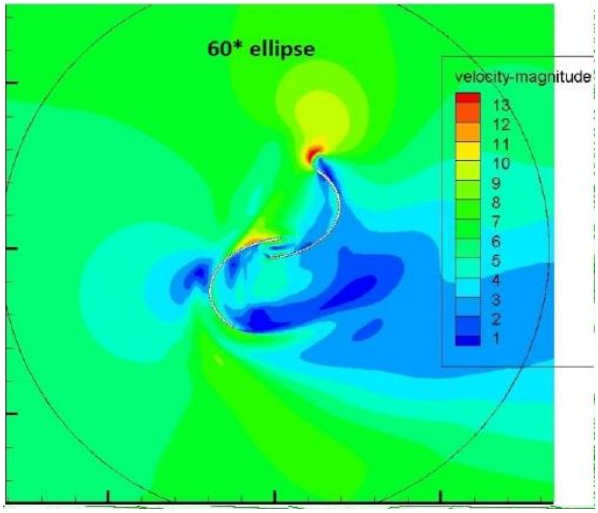

Figure 12: 60° Elliptical profile

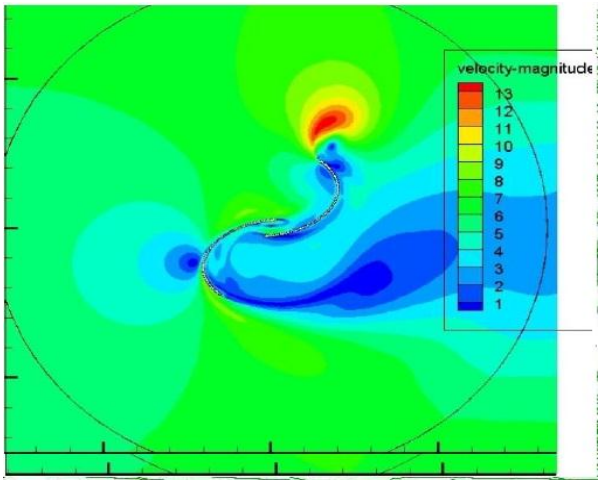

Figure 13: 50° Elliptical profile

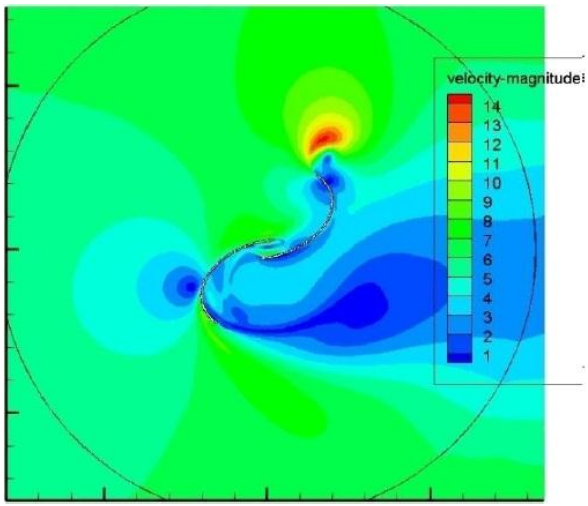

Figure 14: 40° Elliptical profile

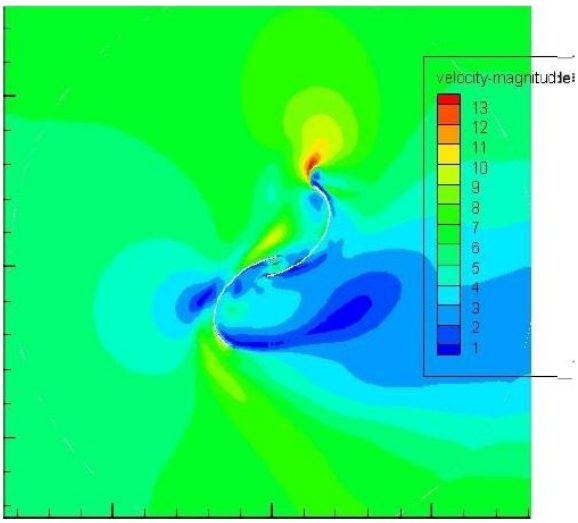

Figure 15: 30° Elliptical profile

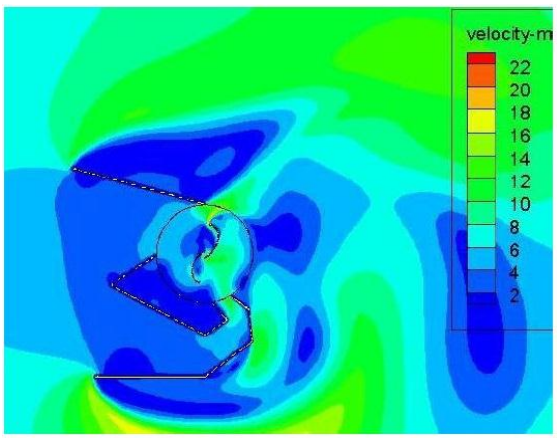

Figure 16: 50° Elliptical profile (Design A)

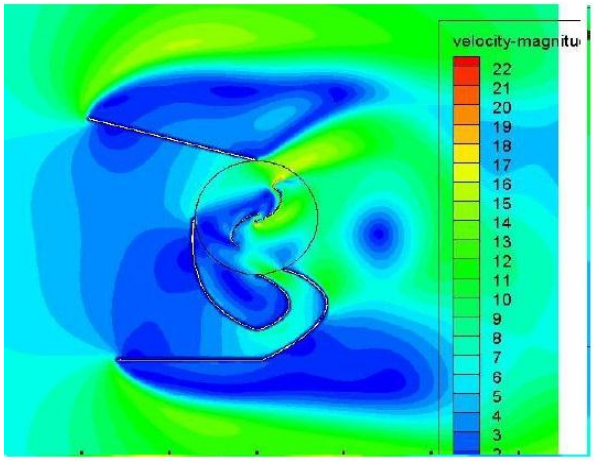

Figure 17: 50° Elliptical profile (Design B)

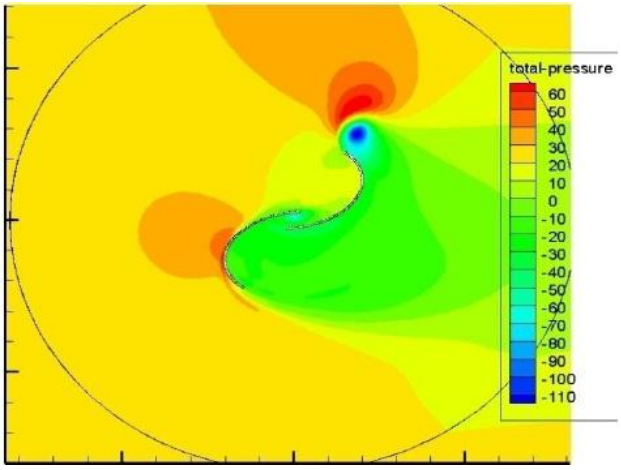

Figure 19: 50° Elliptical profile

Pressure Flow Field (Elliptical Profile)

From the pressure contour it is found that the low pressure region is formed near the advancing blade and a high pressure region is found near the returning blade. The high pressure on the returning blades causes the negative torque generation in the turbine, which adversely affects the power generation capability of the turbine. The negative impact of this pressure is restored to some extent by the returning flow behind the advancing blade which impacts the concave side of the returning blade.

In order to reduce the negative effect of pressure on the returning blade total pressure contours for rotor with guide plate designs were also studied in Fig. 22 and Fig. 23. From the figure, it is clear that pressure difference between the concave and convex sides of blade participates, with the most part of the generated torque. It can be seen that the pressure difference for the design B is higher than design A. The pressure increment on the concave side of returning blade is due to the presence of wind jet which results in higher torque.

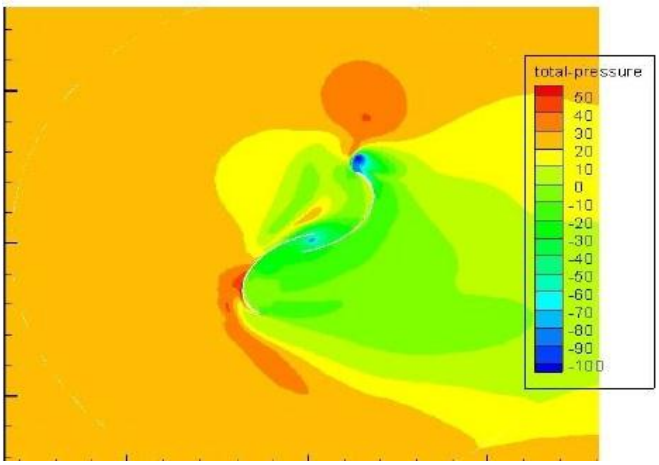

Figure 20: 40° Elliptical profile

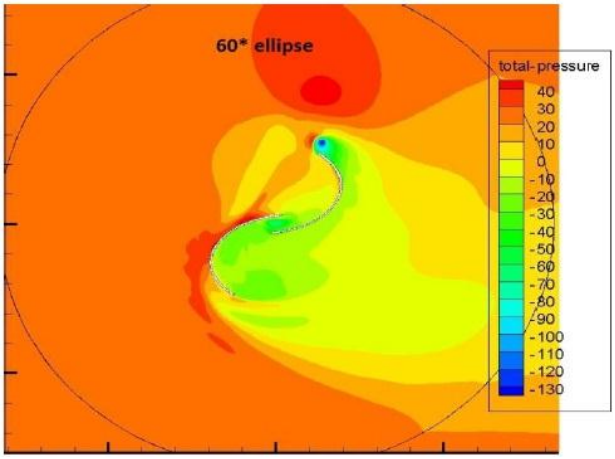

Figure 18: 60° Elliptical profile

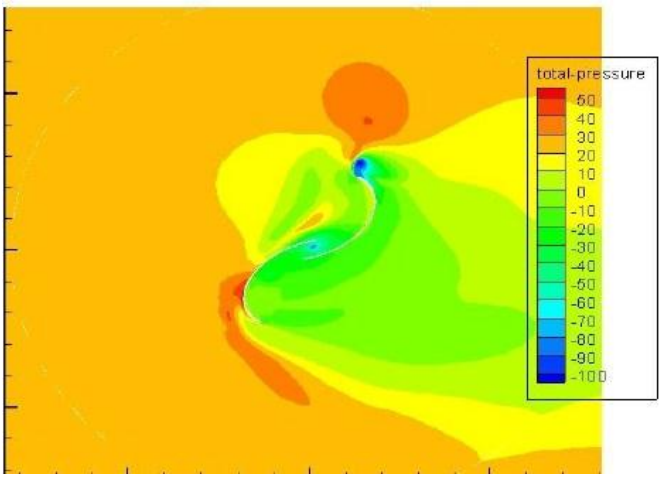

Figure 21: 30° Elliptical profile

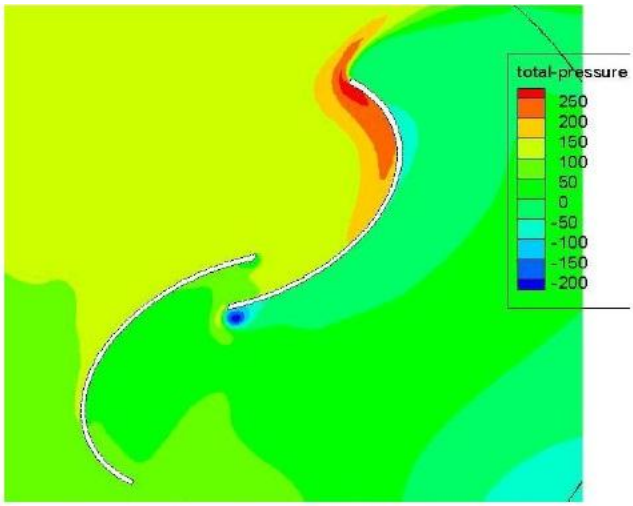

Figure 22: 50° Elliptical profile (Design A)

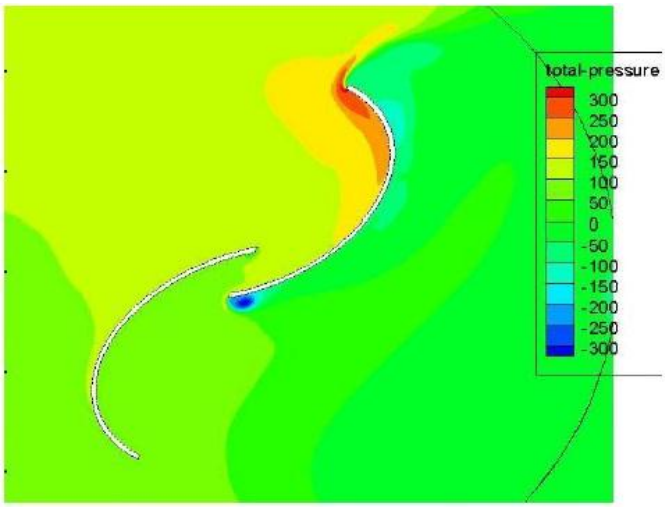

Figure 23: 50° Elliptical profile (Design B)

Velocity Flow Field (Semi-circular and Novel profile)

The velocity distributions at the time when the turbines reached their peak torque with TSR=0.8 has been presented in following figures. The asymmetrical nature of the flow above and below the rotors are evident from the velocity plots which is due to the rotation of the turbine. Another important observation is the recirculation on the concave side of advancing blade. The recirculation flow plays a vital role in the performance of turbine. Moving the recirculation down stream enhances the performance of the rotor i.e., the flow needs to be attached to the walls of the rotor blades as long as possible in order to get better performance. Another important phenomena is the overlap flow. It is the flow through overlap gap ratio of the rotor. The velocity of the overlap flow is responsible for pushing the returning blade in advancing direction especially when rotor is experiencing minimum torque.

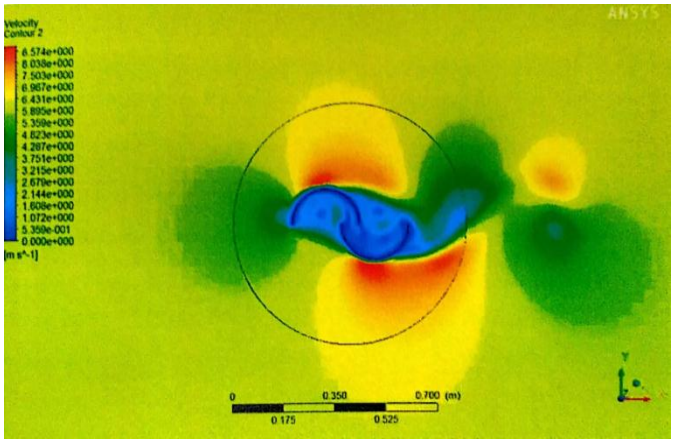

Figure 24: Velocity contour of semicircular profile at 90 degree

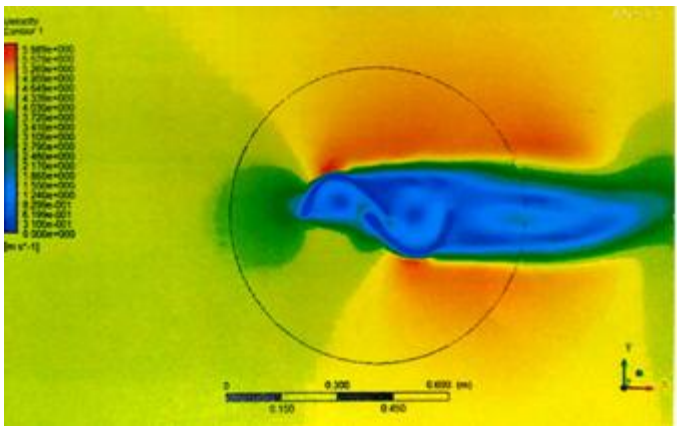

Figure 25: Velocity contour for novel shaped profile at 90 degree

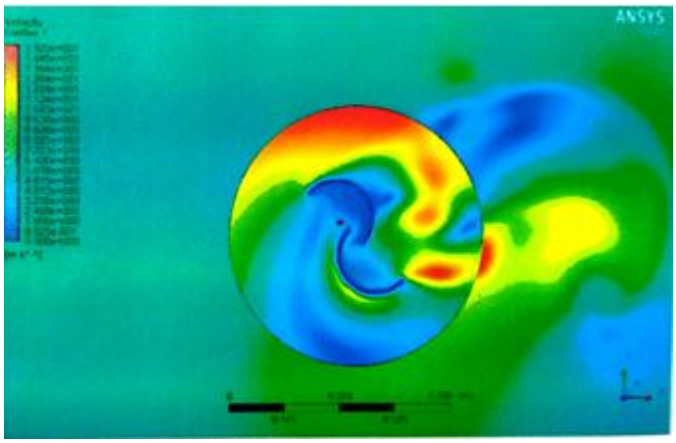

Figure 26: Velocity contour of semicircular profile

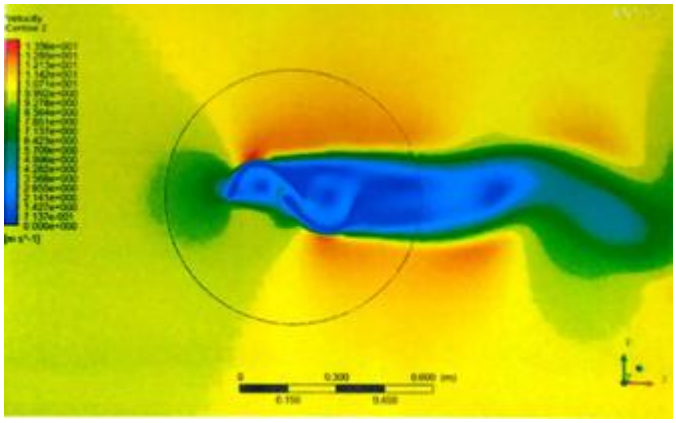

Figure 27: Velocity contour for novel shaped profile

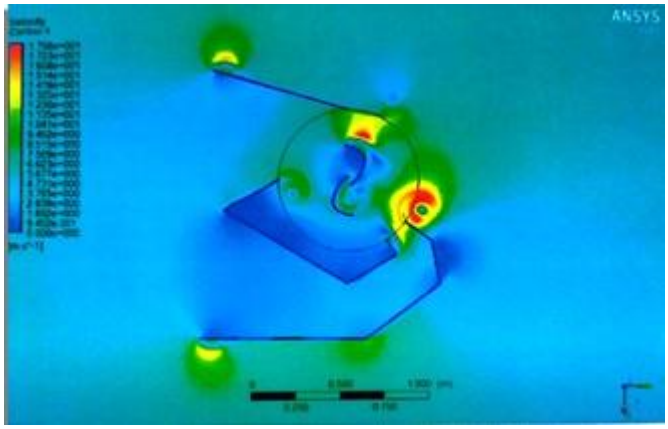

Figure 28: Velocity contour for novel shaped profile with guide vanes design

Pressure Distribution Analysis

The total pressure distribution of semi-circular and novel shape blade with design A and B has been studied. The total pressure contours of these profiles can be seen in the Fig 29, Fig 30, Fig 31 and Fig 32 respectively. From the pressure contour it can be seen that pressure after the blade profile has been decreased.

From the pressure contour it can also be seen that pressure range in the novel shaped profile is higher as compared to that of semi-circular profile. On using guide plates this range of pressure further increases, this results in the increase of coefficient of torque and coefficient of power. Further these guide plates also restrict the incoming air to strike the returning blade directly that reduces the negative torque and results in increment in coefficient of power and torque. These results can also be verified from the graph shown in Fig. 33 and Fig. 34.

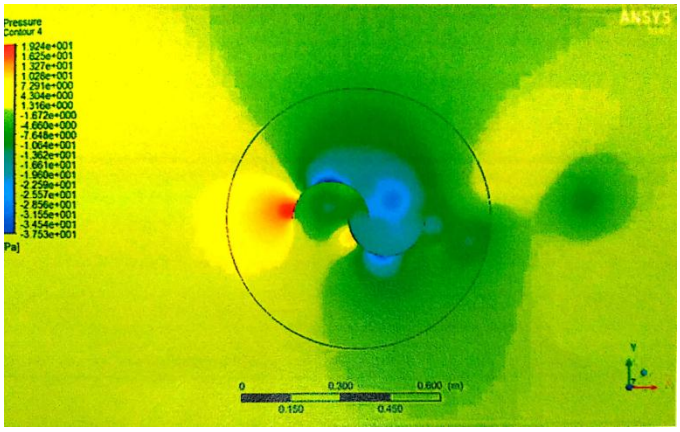

Figure 29: Pressure contour for semicircular profile at 90 degree

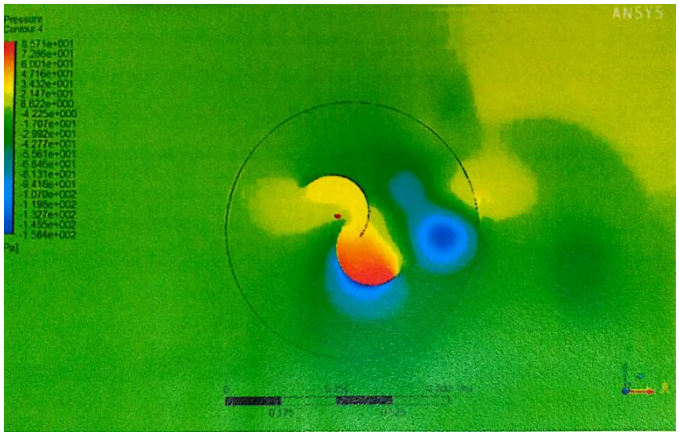

Figure 30: Pressure contour for semicircular profile

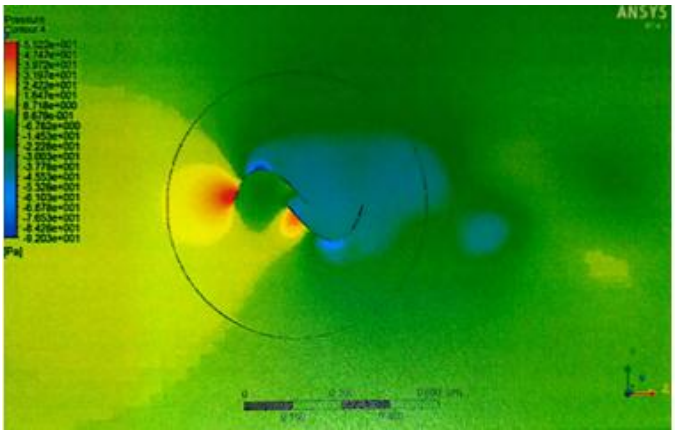

Figure 31: Pressure contour for novel shaped profile at 90 degree

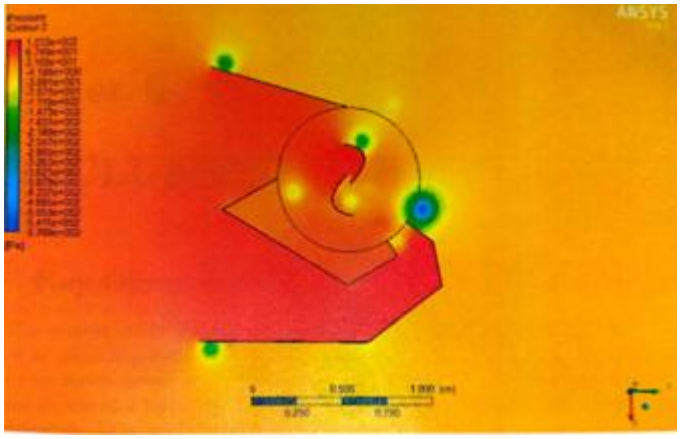

Figure 32: Pressure contour for novel shaped profile with guide vanes design

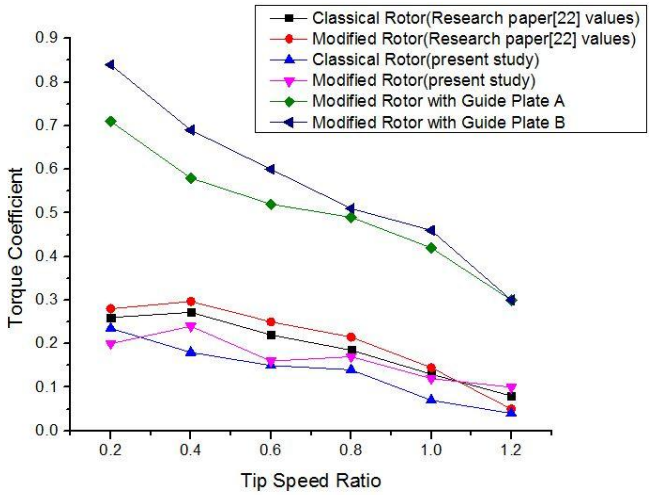

Figure 33: Variation of Torque Coefficient with Tip Speed Ratio for different blade profile

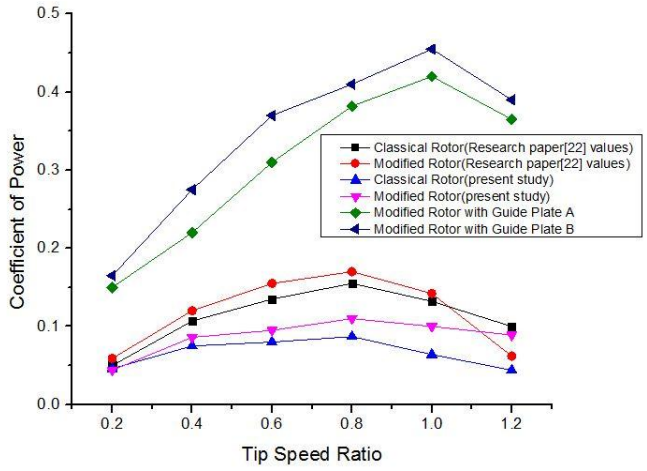

Figure 34: Variation of Power Coefficient with Tip Speed Ratio for different blade profile

CONCLUSION

The 50° elliptical- bladed savonius rotor is more efficient as compared to other elliptical blade profile having same chord length.

The use of guide plates helps in reducing the negative torque of the returning blade which results in the increment of the power coefficient.

The result showed that a new design with curved passage shape has the best performance, with noticeable effects of the wind speed on its performance.

The strong vortex shedding and wide wake generated around and behind the new designs needs more attentions from the point of view of noise generation and dynamic loads in the design of wind turbine farm.

The modified novel savonius rotor is more efficient as compared to classical blade profile having same chord length.

The maximum coefficient of power of modified blade profile without using any guide plate is 0.11 and the value achieved is in the TSR 0.7-0.9.

With the use of guide plates, it has been possible to increase the speed of the wind entering the rotor, without changing the original shape of the rotor.

REFERENCES

[1] Al-Bahadly I, 2009, Building a wind turbine for rural home, Energy for Sustainable Development, vol. 13, pp. 159- 165.

[2] Afungchui D, Kamoun B, Helali A, 2010, The unsteady pressure field and the aerodynamic performances of a Savonius rotor based on the discrete vortex method, *Renewable Energy,* vol. 35, pp. 307-313.

[3] Akwa JV, Junior GA S, Petry AP, 2012, Discussion on the verification of the overlap ratio influence on performance coefficients of a Savonius wind rotor using computational fluid dynamics, *Renewable Energy*, vol. 38, pp. 141-189.

[4] Akwa JV, Vielmo HA, Petry AP, 2012, A review on the performance of Savonius wind turbines, *Renewable and Sustainable Energy Reviews*, vol. 16, pp. 3054-3064.

[5] Altan BD, Atilgan M, 2008, An experimental and numerical study on the improvement of the performance of Savonius wind rotor, *Energy Conversion and Management*, vol. 49, pp. 3425-3432.

[6] Altan B D, Atilgan M, 2010, The use of a curtain design to increase the performance level of a Savonius wind rotors, *Renewable Energy*, vol. 35, pp. 821-829.

[7] Banerjee A, Roy S, Mukherjee P, Saha UK, 2014, Unsteady flow analysis around an Elliptic-Bladed Savonius-style wind turbines. ASME *Gas Turbine India Conference* 2014-814.

[8] Chauvin A, and Benghrib D, 1989, Drag and lift coefficient evolution of a savonius rotor, *Experiments in Fluids*, vol. 8, pp. 118-120.

[9] D˝Alessandro V, Montelpare S, Ricci R, Secchiaroli A, 2010, Unsteady aerodynamics of a Savonius wind rotor: a new computational approach for the simulation of energy performance. *Energy*, vol. 35, pp. 3349-63.

[10] Fernando MSUK, Modi VJ, 1989, On the performance of the Savonius wind turbine, *ASME Journal of Solar Energy Engineering*, Vol.111, pp. 71-81.

[11] Fernando MSUK, Modi VJ, 1993, Unsteady aerodynamics and wake of the Savonius wind turbine: a numerical study, *Journal of Wind Engineering and Industrial Aerodynamics,* vol.46 -47, pp. 811-816.

[12] Jaohindy P, Mctavish S, François Garde, 2013, An analysis of the transient forces acting on Savonius rotors with different aspect ratios, *Renewable Energy*, vol. 55, pp. 286-295.

[13] Kacprazak k, *Liskeiwicz G,* Sobczak K, 2013, Numerical investigation of conventional and modified Savonius wind turbines, *Renewable Energy*, vol. 60, pp. 578-588.

[14] Kamoji MA, Kedare SB, Prabhu V, 2009. Performance test on helical Savonius rotor, *Renewable Energy*, vol. 34, pp. 521-529.

[15] Menet JL, 2004. A double-step Savonius rotor for local production of electricity: a design study, *Renewable Energy*, vol. 29(11), pp. 1843-62.

[16] Mohamed MH, Janiga G, Thévenin D, 2011, Optimal blade shape of a modified Savonius rotor using an obstacle shielding the returning blade, *Energy Conversion and Management*, vol. 52, pp. 236-242.

[17] Nag, P.K. (2010) Power plant engineering, Third edition, Tata McGraw Hill Education Private Limited, P-912.

[18] Paraschivoiu I, 2002, Wind turbine design: with emphasis on Darrieus concept, Presses Inter Polytechnique, Canada.

[19] Ross I and Altman A, 2011, Wind tunnel blockage corrections: review and application to Savonius vertical-axis wind turbines, *Journal of Wind Engineering and Industrial Aerodynamics*, vol. 99, pp. 523-38.

[20] Roy S, Saha UK, 2013, Review on the numerical investigations into the design and development of Savonius wind rotors*, Renewable and Sustainable Energy Reviews*, vol. 24, pp. 73-83.

[21] Roy S, Saha U K, 2014. Design of Savonius-style wind turbines, *In John Abraham Small Scale Wind Power - Design, Analysis, and Economic Impacts, Momentum press,* New York, USA pp. 67- 93.

[22] Nilavarasan Tand Dheenadhayalan J. Numerical investigation of savonious wind turbines with modified blade configurations. International Conference on Energy System and Developments, 21, 2015.